

Urban Heat Island Amplification Estimates on Global Warming Using an Albedo Model

Alec Feinberg

Key Words: Urban Heat Islands, Albedo Modeling, UHI Amplification Effects, Global Warming Causes and Amplification Effects, UHI Footprint, UHI Heat Dome, Cool Roofs, Sea Ice and Moisture Feedbacks

Abstract In this paper we provide nominal and worst case estimates of radiative forcing due to UHI effect (including urban areas) using a Weighted Amplification Albedo Solar Urbanization (WAASU) Model. This is done with the aid of reported findings from UHI footprint and heat dome studies that simplified estimates for UHI amplification factors. Using this method, we find between 1.6 and 7.5% of global warming may be due to the UHI effect (with urban areas). These values may increase to between 5 and 24% when rough climate feedbacks values are estimated. The model also found that the effect was proportional to the UHI amplification area coverage with an area sensitive estimate of about $0.095 \text{ (W/m}^2\text{)/}\%$ Normalized Area. This value perhaps increases to $0.3 \text{ W/m}^2\text{/}\%$ Normalized Area when rough climate feedbacks values are considered. The model is additionally used to quantify an assessment of sea ice feedback warming. Results provide insight into the UHI area effects from a new perspective and illustrates that one needs to take into account effective UHI amplification factors when assessing UHI’s warming effect on a global scale. Lastly, such effects likely show a persuasive argument for the need of world-wide UHI albedo goals.

1 Introduction

It is concerning that there are so few UHI publications recently on their possible influences to global warming. Part of the motivation for this paper is to illustrate the continual need for more up-to-date related studies including UHI amplification effects (that include their urban areas) as will be discussed in this paper. The subject of UHI effect having significant contributions to global warming is very important and should remain so. The topic has a controversial history. One such paper, McKittrick and Michaels (2007) found that the net warming bias at the global level may explain as much as half the observed land-based warming. This study was criticized by Schmidt (2009) and defended for a period of about 10 years by Mckitrick (see McKittrick Website). Other authors have also found significance (Zhao, 1991; Feddema et al., 2005; Ren et al., 2007, 2008; Jones et al., 2008; Stone, 2009; Zhao, 2011; Yang et al. 2011, and Haung et al. 2015). These studies used land-based temperature station data to make assessments. Although the studies have all found global warming UHI significance with different assessments, they have yet to influence the IPCC enough to necessitate albedo recommendations in their many reports and meetings like the CO₂ effort. This is important because we feel the IPCC’s should be more proactive in helping the global community recognizing the need for UHI albedo guidelines. Although the IPCC have provided reports on UHIs including health related issues, the response to their reports does not appear to be effective on the global scale compared with the on-going CO₂ effort.

The contention that UHI effects are basically only of local significance is most likely related to urban area estimates. For example, IPCC (Satterthwaite et. al. 2014) AR5 report references Schneider et al. (2009) study that resulted in urban coverage of 0.148% of the Earth (Table 1). This seemingly small area tends to dismiss the contention that UHI effect can play a large scale role in global warming. Furthermore, estimates of how much of land has been urbanized vary widely in the literature and this is in part due to the definition of what is urban and the datasets used. Although, such estimates are important for environmental studies, obtaining true estimates for the small urbanized area relative to the total land is apparently very difficult. This is compounded by the fact that there is a significant difference in how groups define the term ‘urban’. Thus, urbanized surface area land approximations vary widely and most are obtained with satellite measurements sometimes supplemented in some way with census data. Table 1 captures the variations from some papers that are of interest.

Table 1. Urbanization area extent estimates from various sources

Percent of Land	Percent of Earth	References
2.7	0.783	GRUMP, 2005 - using NASA satellite light studies based on 2004 data and supplemented with census data
1%	0.29	NASA, 2000; Galka, 2016 – from satellite data
0.51	0.148	Schneider et al. 2009 - based on 2000-2001 data and referenced in the IPCC report (Satterthwaite, 2014)
0.5%	0.145	Zhou 2015 - based on a 2000 data set

56
57 In addition, global warming UHI amplification effects have not been quantified to a large degree related to area
58 estimates. Urbanized average solar areas remain unknown.

59
60
61 In our study, one key paper listed in the Table 1 is due to Schneider et al. (2009) since it is cited by the AR5 2014
62 IPCC report (Satterthwaite et al. 2014). In Schneider’s paper, the larger area found in the GRUMP 2005 study
63 (Table 1) is criticized. These area estimates are of interest in our paper for the *Weighted Amplification Albedo Solar*
64 *Urbanization (WAASU) Model*. As well, the Amplification factors we use are related to their urban coverage
65 estimates. In this paper we use both the Schneider et al. and GRUMP studies for the nominal and worst cases
66 urbanization area estimates respectively. Furthermore, they were both done using data sets from around 2000 which
67 is a convenient time to extrapolate down to 1950 and up to 2019 (see Sec. 3).

68
69 In our study, where we introduce the WAASU model, we will see that it has some advantages over the ground-based
70 temperature studies like McKittricks and Michaels. The model is non probabilistic, in line with the way typical
71 energy budgets are calculated. It uses only two key parameters (effective area and average albedo). Because it is
72 simplistic, it has transparency compared with the complex land-based studies.

73
74 **1.1 UHI Amplification Effects**

75
76 The table below lists the global warming causes and amplification effects. In this section we will summarize only
77 the UHI amplification effects listed in the table since the root causes and the main global warming feedback
78 amplification effects are fairly well known.

79
80 **Table 2.** Global warming cause and effects

Global Warming Causes →	Population → Expanding Urban Heat Islands (UHI), Roads & Increases in Greenhouse Gas
Global Warming Feedback Amplification Effects →	Water Vapor Feedback, Land Albedo Change Due to Cities & Roads, Ice and Snow –Albedo Feedback, Lapse Rate Feedback, Cloud Feedback, etc.
Urban Heat Island Amplification Effects →	UHI Solar Heating Area (Building Areas), UHI Building Heat Capacities, Humidity Effects and Hydro-Hotspots, Reduced Wind Cooling, Solar Canyons, Loss of Wetlands, Increase in Impermeable Surfaces, Loss of Evapotranspiration Natural Cooling.

81
82 The UHI amplification effects that we consider to dominate listed in the table are as follows:

- 83
84 • **The humidity amplification effect:** This has been observed. For example, Zhao et al. (2014) noted that UHI
85 temperature increases in daytime ΔT by 3.0°C in humid climates but decreasing ΔT by 1.5°C in dry
86 climates. They noted that such relationships imply that UHIs will exacerbate heat wave stress on human
87 health in wet UHI climates. One explanation for this is how heat dissipates through convection which is
88 more difficult in humid climates. Another explanation is that warmer air holds more water vapor. This can
89 increase local specific humidity so that there could be local greenhouse effects.
- 90
91 • **The heat capacity and solar heating area amplification effect:** This contributes to the day-night UHI
92 cycle. Here in most cities, it is observed that daytime atmospheric temperatures are actually cooler
93 compared to night. For example, in a study by Basara et al. (2008) in Oklahoma city UHI it was found that
94 at just 9-m height, the UHI was consistently 0.5–1.75°C greater in the urban core than the surrounding rural
95 locations at night. Further, in general UHI impact was strongest during the overnight hours and weakest
96 during the day. This inversion effect can be the results of massive UHI buildings acting like heat sinks,
97 having giant heat capacities and storing heat in their reservoir via convection as solar radiation is absorbed
98 during the day. This often reduces the UHI day effect, but at night buildings cools down, giving off their
99 stored heat that increases local temperatures to the surrounding atmosphere. This effect increases with city
100 growth as buildings have gotten substantially taller (Barr 2019) since 1950.
- 101
102 • **The hydro-hotspot amplification effect:** This effect is not well addressed. Here atmospheric moisture
103 source is a complex issue due to Hydro HotSpots (HHS). Hydro hotspots occur when buildings are hot due
104 to sun exposure. Then during precipitation periods, the hot highly evaporation surfaces increase localized
105 water vapor in the air via the effect that warm air holds more moisture. This increase in local greenhouse
106 gas, could blanket city heat and increase infrared radiation during these periods. This, as discussed above,
107 is another possible UHI humidity amplification.

- 109 • **Reduced wind cooling and solar canyons:** In UHIs reduced wind is a known effect due to building wind
 110 friction which inhibits cooling by convection. As well, tall buildings create solar canyons and trap sunlight
 111 reducing the average albedo although some benefits occurs from shading. In general, both have the effect
 112 of amplifying the temperature profile of UHIs.

113

114 **2 Data and Methods**

115

116 We see from the previous section that estimating climate change impact just based on the UHI and Urban area
 117 coverage as in Table 1, cannot take into account solar heating building sidewall areas, massive heat capacities, the
 118 humidity effects, wind reduction and the solar canyon effect which amplify UHI effects beyond its own climate area.

119 **2.1 UHI Area Amplification Factor**

120

121 In order to estimate the UHI amplification effects, it is logical to first look at UHI footprint (FP) studies as they
 122 provide some measurement information. Zhang et al. (2004) found the ecological footprint of urban land cover
 123 extends beyond the perimeter of urban areas, and the footprint of urban climates on vegetation phenology they found
 124 was 2.4 times the size of the actual urban land cover. In a more recent study by Zhou et al. (2015), they looked at
 125 day-night cycles using temperature difference measurements. In this study they found UHI effect decayed
 126 exponentially toward rural areas for majority of the 32 Chinese cities. Their study was very thorough and extended
 127 over the period from 2003 to 2012. They describe China as an ideal area to study since it has experienced the
 128 rapidest urbanization in the world in the decade they evaluated. They found that the “footprint” of UHI effect,
 129 including urban areas, was 2.3 and 3.9 times of urban size for the day and night, respectively. We note that the
 130 average day-night amplification footprint coverage factor is 3.1.

131 Looking at Table 2, we see that the UHI Amplification Factor (AF_{UHI}) is highly complex making it difficult to assess
 132 from first principles as it would be some function of Table 2 components:

$$133 \quad AF_{UHI \text{ for } 2019} = f\left(\overline{Build}_{Area} \times \overline{Build}_{C_p} \times \overline{R}_{wind} \times \overline{LossE}_{vtr} \times \overline{Hy} \times \overline{S}_{canyon}\right) \quad (1)$$

134 were

135 \overline{Build}_{Area} = Average building solar area136 \overline{Build}_{C_p} = Average building heat capacity137 \overline{R}_{wind} = Average city wind resistance138 \overline{LossE}_{vtr} = Average loss of evapotranspiration to natural cooling & loss of wetland139 \overline{Hy} = Average humidity effect due to hydro-hotspot140 \overline{S}_{canyon} = Average solar canyon effect

141

142 As a helpful example, one basic formulation that might be suggested is a product of power law average ratios over
 143 all urban cities compared to a reference year (1950) such that

144

$$145 \quad AF_{UHI \text{ for } 2019} = \left(\frac{(\overline{Build}_{Area})_{2019}}{(\overline{Build}_{Area})_{1950}}\right)^{N_1} \left(\frac{(\overline{Build}_{C_p})_{2019}}{(\overline{Build}_{C_p})_{1950}}\right)^{N_2} \left(\frac{(\overline{R}_{wind})_{2019}}{(\overline{R}_{wind})_{1950}}\right)^{N_3} \left(\frac{(\overline{LossE}_{vtr})_{2019}}{(\overline{LossE}_{vtr})_{1950}}\right)^{N_4} \left(\frac{(\overline{Hy})_{2019}}{(\overline{Hy})_{1950}}\right)^{N_5} \left(\frac{(\overline{S}_{canyon})_{2019}}{(\overline{S}_{canyon})_{1950}}\right)^{N_6} \cdot (2)$$

146

147 In order to provide some estimate of this factor, we note that Zhou et al. (2015) found the FP physical area (km^2),
 148 correlated tightly and positively with actual urban size having correlation coefficients higher than 79%. This
 149 correlation can be used to provide an initial estimate of this complex factor. Area estimates have been obtained in
 150 the next Section in Table 3 between 2019 and 1950 time frames. These yield the following results for the Schneider
 151 et al. (2009) and the GRUMP (2005) extrapolated area results:

$$152 \quad AF_{UHI \text{ for } 2019} = \frac{(\text{Urban Size})_{2019}}{(\text{Urban Size})_{1950}} \approx \begin{cases} \left(\frac{[0.188]_{2019}}{[0.059]_{1950}}\right)_{\text{Schneider}} = 3.19 \\ \left(\frac{[0.952]_{2019}}{[0.316]_{1950}}\right)_{\text{GRUMP}} = 3.0 \end{cases} \quad (3)$$

153 Between the two studies, the UHI area amplification factor average is 3.1. Coincidentally, this is the same factor
 154 observed in the Zhou et al. (2015) study for the average footprint. This factor may seem high. However, it is likely
 155 conservative. There are other effects that would be difficult to assess. For example, increases in global draught due
 156 to loss of wet lands, deforestation effects due to urbanization and draught related fires. It could also be important to
 157 factor in changes of other impermeable surfaces since 1950 such as highways, large impermeable surfaces (parking
 158 lots and event centers), and so forth.

159
 160 **2.2 Alternate Method Using the UHI’s Horizontal Extent**
 161

162 An alternate approach to check the estimate of Equation 3, is to look at the UHI’s horizontal extent. Fan et al. (2017)
 163 using an energy balance model to obtain the maximum horizontal extent of a UHI heat dome in numerous urban
 164 areas found the nighttime extent of 1.5 to 3.5 times the diameter of the city’s urban area (2.5 average) and the
 165 daytime value of 2.0 to 3.3 (2.65).

166
 167 Applying this energy method (instead of the area ratio factor in Eq. 3), yields a diameter in 2019 compared to that of
 168 1950 increase of about 1.8. This implies a factor of $2.5 \times 1.8 = 4.5$ higher in the night and $2.65 \times 1.8 = 4.8$ in the day in
 169 1950 (average 4.65). This increase occurs 62.5% of the time according to Fan et al., (where their steady state
 170 occurred about 4 hours after sunrise and about 5 hours after sunset) yielding an effective UHI acceleration factor of
 171 2.9. We note this acceleration factor is in good agreement with Equation 3. The fact that it is a bit lower may be
 172 because Fan et al. only assessed the steady state region, one would anticipate some increase from the non-steady
 173 state period.

174
 175 **2.3 Area Extrapolations for 1950 and 2019**
 176

177 In order to assess the urbanized area, (also used in determining the UHI amplification factor ratios above), we need
 178 to project the Schneider and GRUMP area estimates down to 1950 and up to 2019. Both use datasets from around
 179 2000 so this is a convenient somewhat middle time-frame. Here we decided to use the world population growth rate
 180 (World Bank 2018) which varies by year as shown in Appendix A in Figure A1. We used the average growth rate
 181 per ½ decade for iterative projections (about 1.3% to 1.6% per year).

182
 183 To justify this we see that Figure A2a illustrates that building material aggregates (USGS 1900-2006) used to build
 184 cities and roads correlates well to population growth (US Population Growth 1900-2006).

185
 186 **Table 3.** Extrapolated and amplified urbanized coverage estimates

Year	Urban coverage percent of Earth	Amplification factor effect	Effective amplification coverage area effect
Schneider study			
1950	0.059*	1	0.059%
2000-2001	$0.0051 \times 29\% = 0.148$		
2019	0.188*	3.1 AF _{UHI} **	0.583%
Worst case GRUMP study			
1950	0.316%*	1	0.316%
2000	$0.027 \times 29\% = 0.783\%$		
2019	0.952%*	3.1 AF _{UHI} **	2.95%

187 *Growth rate of cities using world population yearly growth rate in Fig A1, **AF_{UHI} is the area
 188 amplification factor for 2019 referenced to 1950.
 189

190 It is also interesting to note that building materials for cities and roads also correlates well to global warming trends
 191 (NASA 1900-2006) shown in Figure A2b.

192
 193 Column 2 in Table 3 show the projections with the actual year (~2000) data point tabulated value also listed in the
 194 table (also see Table 1). The UHI area amplification factor of 3.1 (Column 3) are then applied to Schneider and
 195 GRUMP studies shown in Column 4.

198 **2.4 Weighted Amplification Albedo Solar Urbanization (WAASU) Model Overview**

199
200 The WAASU model is very straightforward; it is based on a global weighted albedo model. The Earth Albedo is
201 given by

202
$$Earth\ Albedo = \sum_i \{ \%Effective\ Surface\ Area_i \times Surface\ Item\ Albedo_i \} + Cloud\ Area \times Cloud\ Albedo. \quad (4)$$

203 Here the effective surface area is given by

204
205
$$Effective\ Surface\ Area = Surface\ Area \times \%Solar\ Irradiance. \quad (5)$$

206
207 We note that the change in the Earth Albedo over time (from 1950 to 2019), is just a function of the UHI area
208 variation, (when holding all unrelated UHI components fixed), that is

209
210
$$\left(\frac{dEA}{dt} \right)_{EA'} = \sum_i \left(Albedo_{UHI} \times Solar\ Irradiance \times \frac{dArea_{UHI}}{dt} \right)_i, \quad (6)$$

211 where EA is the Earth Albedo, and EA' are all other Earth components (held fixed). Although it is possible that the
212 solar irradiance percent changes due to new city locations, in this model we assume it is fixed at 100%. This
213 indicates, for example, that even if we were to change the *Effective Surface Area* of perhaps the *sea ice component*
214 due to the fact that it receives about 40% irradiance compared with other areas and redistributed its radiance (per the
215 Earth's energy budget), it would not affect the overall results when looking at the albedo change from 1950 to 2019.
216 Therefore, the model allows freedom to only work with area coverage changes when focusing on the UHI effect. On
217 the other hand, sea ice solar irradiance comes into play when we are considering its global albedo effect from 1950
218 to 2019 (see Appendix C). However, the solar radiation weighting, albedo, and areas for all Earth components are
219 subjected to the constraints below.

220
221
222 **2.4.1 Model Constraints**

223
224 This model is subject to the constraint

225
$$Total\ Area = \sum_i \{ \%Earth\ Surface\ Areas_i \} + \%Cloud\ Area = 100\% \quad (7)$$

226
227 and the normalization constraint for the Earth surface areas (when the UHI area is increased) must then be subject to

228
229
$$\sum_i \{ \%Earth\ Surface\ Areas_i \} = 100\% - \%Cloud\ Area. \quad (8)$$

230
231 To simplify things as much as possible, only five Earth constituents are used: *water*, *sea ice*, *land*, *UHI coverage*,
232 *and clouds* (where *land* is its area minus the UHI coverage). These components are fairly easy to estimate and
233 references for their values are provided in Appendix D. Furthermore, we use consistent values found in the IPCC
234 AR5 report (Hartmann et al., 2013) assessment of the Earth's energy budget for solar irradiance. Table 4
235 summarizes the constraints from these IPCC values.

236
237 The fixed components of our model maintain relative consistency from 1950 to 2019. The non-fixed value is the
238 urban coverage as indicated by Equation 6. The only unknown value is the *land* albedo (minus the UHI coverage)
239 and this value is adjusted to obtain the IPCC global albedo of 29.4118% and its *land* value of incident/reflected
240 value of 7.0588.

241 **Table 4. IPCC Earth energy budget values (Hartmann et al., 2013)**

IPCC Item	Incident and Reflected Radiation (W/m ²)	Albedo %	Absorbed (W/m ²)
Earth	100/340	29.4118	240=340x(1-.294)
Atmosphere & Clouds	76/340	22.3529	79
Earth Surface Albedo	24/340	7.0588	161

242
243

244 These values are used as a 1950 starting point and then the 2019 increase for UHI coverage area is inserted. This
 245 increases the Earth’s area to greater than 100%. Therefore, renormalization is done per the constraint of Equation 8
 246 (detailed in Appendix B).

247
 248 **3 Results and discussion**
 249

250 Using the extrapolated area coverage in Table 3 with the 3.1 amplification factor applied to the urbanized growth,
 251 the resulting global albedo change occurred of 29.3956% in 2019 (Table 5b) compared to the earlier 1950 albedo
 252 value of 29.4118% (Table 5a) for the Schneider nominal case. As well, for the GRUMP worst case, the albedo
 253 changed from 29.4118% (Table 6a) to 29.3322% (Table 6b) due to the urbanized growth.

254
 255 As we mentioned earlier, the increases in the solar surface area of the Earth, which will occur with city growth of
 256 tall buildings and their solar areas, however comparatively small, requires renormalization in the model of the Earth
 257 surface components of the WAASU model (detailed in Appendix B). This is displayed in column 3 in Tables 5b and
 258 6b. While the model is sensitive to urban coverage changes, it works well with renormalization showing a high level
 259 of consistency to urban coverage proportionality changes. This is indicated in Table 7 where we find the GRUMP
 260 2019 area sensitivity is 0.0944%Norm Area/(W/m²) (=0.271/2.87) compared with the Schneider area sensitivity of
 261 0.0948 %Norm Area/(W/m²) (=0.055/0.58).

262
 263 **Table 5a.** Schneider results (Albedo=29.4118, 1950) **Table 5b.** Schneider results (Albedo=29.3956%, 2019)

Surface	Albedo	% Area of Surface	Normalized Earth Area	Weighted Albedo %
	A	B	C=A x B x (1-0.67)	A x C
Sum of Water Type		71		
Sea Ice	0.6	15	4.95	2.970
Water	0.06	56	18.48	1.109
Sum of Land Type		29		
Land - (UHI + Coverage)	0.3118	28.941	9.55053	2.978
UHI + Coverage	0.12	0.059	0.01947	0.002
		Σ=100.000	33.000	7.05882
			Cloud Area	
Clouds	0.3336	67	67	22.35294
Σ Sum Earth %			100.000	
Σ Global Albedo				29.4118

Surface	Albedo	Normalized % Surface Area	Normalized Earth Area	Weighted Albedo %
	A	B	C=A x B x (1- 0.67)	A x C
Sum of Water Type		70.6298		
Sea Ice	0.6	14.9218	4.924194	2.955
Water	0.06	55.7081	18.383673	1.103
Sum of Land Type		29.37		
Land - (UHI + Coverage)	0.3118	28.79	9.5007	2.962
UHI + Coverage	0.12	0.58	0.1914	0.023
		Σ=100.000	33.000	7.0197
			Cloud Area	
Clouds	0.3336	67	67	22.3529
Σ Sum Earth %			100.000	
Σ Global Albedo				29.3956

264

265 **Table 6a.** GRUMP results (Albedo=29.4118, 1950) **Table 6b.** GRUMP results (Albedo=29.3322%, 2019)

Surface	Albedo	% Surface Area	Normalized Earth Area	Weighted Albedo %
	A	B	C=A x B x (1-0.67)	A x C
Sum of Water Type		71		
Sea Ice	0.6	15	4.95	2.970
Water	0.06	56	18.48	1.109
Sum of Land Type		29		
Land - (UHI + Coverage)	0.3135	28.684	9.46572	2.968
UHI + Coverage	0.12	0.316	0.10428	0.013
Sum Surface %		Σ=100.000	33.000	7.0588
			Cloud Area	
Clouds	0.3336	67	67	22.3529
Σ Sum Earth %			100.000	
Σ Global Albedo				29.4118

Surface	Albedo	Normalized % Surface Area	Normalized Earth Area	Weighted Albedo %
	A	B	C=A x B x (1- 0.67)	A x C
Sum of Water Type		69.1778		
Sea Ice	0.6	14.615	4.82295	2.894
Water	0.06	54.5628	18.005724	1.080
Sum of Land Type		30.8221		
Land - (UHI + Coverage)	0.3135	27.9478	9.222774	2.891
UHI + Coverage	0.12	2.8743	0.948519	0.114
Sum Earth %		Σ=100.000	33.000	6.8655
			Cloud Area	
Clouds	0.3336	67	67	22.3529
Σ Sum Earth %			100.000	
Σ Global Albedo				29.3322

266

267 Table 7 provides a summary of albedo changes found in the WASSU model along with the expected solar long wave
 268 radiation increase. From the above global WAASU model, the estimates of the Earth’s radiated long wavelength
 269 emissions are set equal to the short wave radiation absorption:

270

$$P_{Total} = 340 \text{ W/m}^2 (1 - \text{Albedo}). \tag{9}$$

271

272

273 Then the change from 1950 to 2019 represents the equivalent increase in long wave radiation is given by

274
275
276
277
278
279
280
281

$$\Delta P_{Total} = 340 \text{ W/m}^2 \{ (1-\text{Albedo})_{2019} - (1-\text{Albedo})_{1950} \}. \tag{10}$$

Results are compiled in Table 7. The table also includes “what if” estimates, if we could change urbanization to be more reflective with cool roofs to reverse the effect. The values here are relative to the conservative UHI amplification values.

Table 7. Albedo and radiative increase model results with UHI effective area.

Year	Urban Extent Global Area %	UHI Effective Global Surface % Area	Normalized UHI Effective Global Surface % Area	Albedo Cities	Global Weighted Albedo	ΔP_{Total} UHI Radiative Increase W/m^2 (%GW)*	Sensitivity $\frac{W}{m^2 \cdot K}$	Model Area Sensitivity $\frac{\Delta P_{Total} (W/m^2)}{Norm \% Area}$
Nominal Case IPCC Schneider 2009 Study								
1950	0.059	0.059	0.059	0.12	29.4118	0	—	—
2019	.188	0.583	0.58	0.12	29.3978	0.055 (1.54%)*	0.058	0.0948
What if	0.188	0.583	0.58	0.204	29.4118	-0.055 (-1.54%)*	-0.058	—
Worst Case GRUMP 2005 Study								
1950	0.316%	0.316	0.316	0.12	29.4118	0	—	—
2019	0.952%	2.95	2.8743	0.12	29.3322	0.271 (7.6%)*	0.285	0.0944
What if	0.952%	2.95	2.8743	0.2039	29.4118	-0.271 (-7.6%)*	-0.285	—

*Percent of Warming estimate, $P=340 \times (1-\text{Albedo})$, $\%GW = \{ (P/\epsilon\sigma)^{0.25}_{2019} - (P/\epsilon\sigma)^{0.25}_{1950} \} / 0.95^\circ\text{C}$, $\epsilon=1$

282
283
284
285
286
287
288
289
290
291
292

The general results are summarized:

- Nominal Schneider case from 1950 to 2019 is 0.055 W/m^2 due to urban amplification coverage. This would equate to about 1.55% of global warming assuming the total increase from 1950 is about 0.95°C in 2019.
- Worst GRUMP case from 1950 to 2019 is 0.271 W/m^2 due to urban amplification coverage. This would roughly equate to about 7.5% of global warming assuming the total increase from 1950 is about 0.95°C in 2019.
- “What if” corrective action results of cool roofs indicates that changing city albedos in both the Schneider and the GRUMP case from 0.12 to 0.204 would reverse the increase in emission back to 1950 levels.

293
294
295
296
297
298
299
300
301

Model consistency is indicated in the area sensitivity column in Table 7. Furthermore, we note that radiation increase goes as the area changes. That is, the Schneider to Grump normalized area increase from 0.58 (Schneider) to 2.8743% (GRUMP) yields a factor of 3.96 $(= (2.874 - .58) / .58)$. This can be compared to the observed long radiation increase from 0.055 W/M^2 (Schneider) to 0.271 W/M^2 (GRUMP) that also yields a similar factor of 3.93 $(= (0.271 - .055) / .055)$. This observation along with the area sensitivity values can be helpful in estimating future warming trends due to UHI growth rates, which at the present time from Figure A1, is about 1.2% per year. We also note that in both the Schneider and GRUMP case, implementing cool roof requires the same albedo change from 0.12 to 0.204 in order to reverse the warming trend.

302
303
304
305
306

Although global warming assessment obtained in the WAASU model, especially for the Schneider case does not appear to show much contribution to global warming, we find that climate sensitivity feedback estimates increase the UHI effective contribution significantly. Suggestions in Appendix C indicate that the root cause global warming contribution may go as high as 5% for the Schneider case and 24% for the GRUMP case (see Table C2).

4 Conclusions

307
308
309
310
311
312
313

In this paper we were able to estimate using UHI effect (with urban area) amplification coverage estimates with the aid of estimated UHI amplification factors. These estimates inserted into our WAASU model found that between 0.055 and 0.271 W/m^2 of radiative forcing is possible according the WAASU model (this results indicates that about 1.6 and 7.5% of global warming may be due to the UHI effect (with urban areas). The model found that the effect was proportional to the UHI amplification area coverage with area sensitive estimate was about 0.095

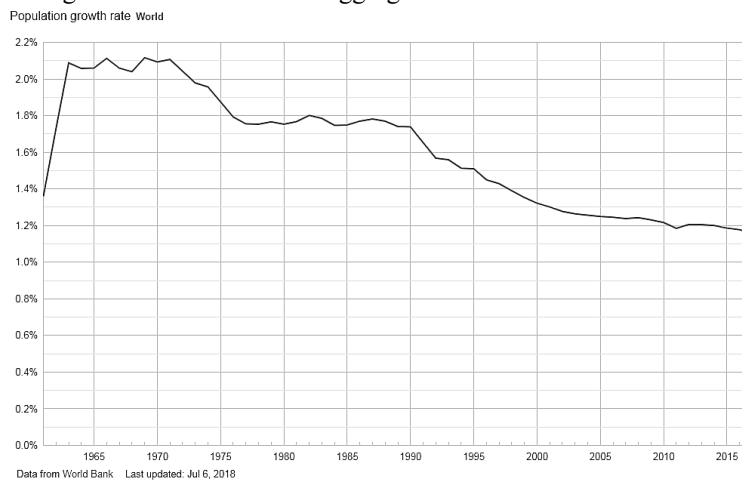
314 (W/m²)/%Normalized Area. Examples are provided in Appendix C to illustrate how the UHI root cause global
 315 warming contribution increase significantly when climate feedback factors are considered. As area estimates and
 316 UHI amplification factors are very sensitive to the final results, it is clear refined values of both would be important
 317 for further study.

318
 319 Below we provide suggestions and corrective actions which include:

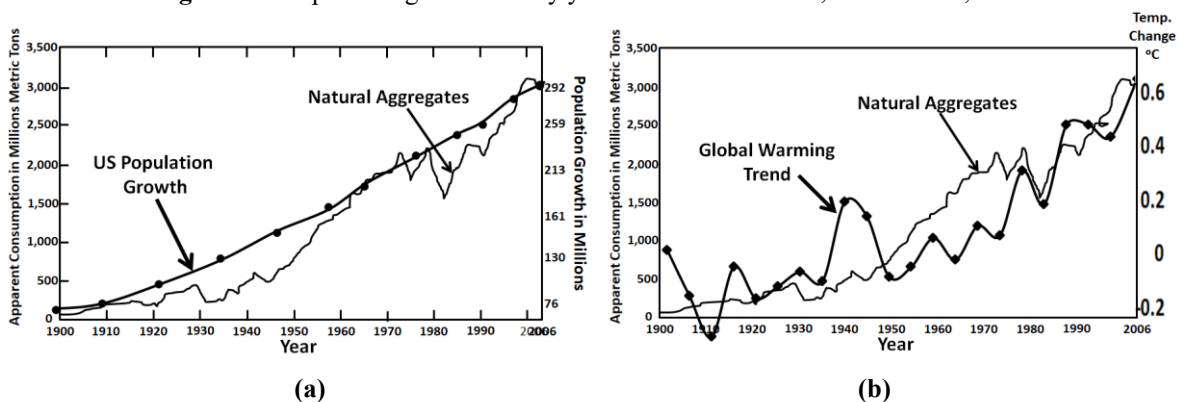
- 320 • IPCC be more proactive in helping to providing albedo guidelines or recommendation similar to their CO₂
 321 effort for both UHIs and roads.
- 322 • A guideline for future albedo design requirements of city and roads should be developed.
- 323 • Recommend an agency like NASA be tasked with finding applicable solutions to cool down UHIs.
- 324 • Recommendation for cars to be more reflective. Here although world-wide cars likely do not embody much
 325 of the Earth's area, recommending that all new manufactured cars be higher in reflectivity (e.g., silver or
 326 white) would help raise awareness of this issue similar to electric cars that help improve CO₂ emissions.

327
 328 **Appendix A: Growth Rates and Information on Natural Aggregates**
 329

330 Below is a plot of the world population growth rate that varies from about 2.1 to 1.1. This is used to make growth
 331 rate estimates of urban coverage. We note that natural aggregate used to build cities and roads are reasonably
 332 correlated to population growth in Figure A2a. Also of interest (Fig. A2b) is the fact that one can see some
 333 correlation to global warming with the use of natural aggregates.



334
 335 **Figure A1.** Population growth rate by year from 1960 to 2018, World Bank, 2018



336
 337 **Figure A2. a)** Natural aggregates correlated to U.S. Population Growth (USGS 1900-2006) **b)** Natural aggregates
 338 correlated to global warming (NASA 2020)
 339

340
 341
 342
 343
 344 **Appendix B: Albedo Model Renormalization Information**
 345

346 Table 5a and b are reproduced to illustrate the renormalization method.
 347

348 **Table 5a.** Schneider results (Albedo=29.4118, 1950) **Table 5b.** Schneider results (Albedo=29.3956%, 2019)

Surface	Albedo	% Area of Surface	Normalized Earth Area	Weighted Albedo %
	A	B	$C=A \times B \times (1-0.67)$	A x C
Sum of Water Type		71		
Sea Ice	0.6	15	4.95	2.970
Water	0.06	56	18.48	1.109
Sum of Land Type		29		
Land - (UHI + Coverage)	0.3118	28.941	9.55053	2.978
UHI + Coverage	0.12	0.059	0.01947	0.002
		$\Sigma=100.000$	33.000	7.05882
			Cloud Area	
Clouds	0.3336	67	67	22.35294
Σ Sum Earth %			100.000	
Σ Global Albedo				29.4118

Surface	Albedo	Normalized % Surface Area	Normalized Earth Area	Weighted Albedo %
	A	B	$C=A \times B \times (1-0.67)$	A x C
Sum of Water Type		70.6298		
Sea Ice	0.6	14.9218	4.924194	2.955
Water	0.06	55.7081	18.383673	1.103
Sum of Land Type		29.37		
Land - (UHI + Coverage)	0.3118	28.79	9.5007	2.962
UHI + Coverage	0.12	0.58	0.1914	0.023
		$\Sigma=100.000$	33.000	7.0197
			Cloud Area	
Clouds	0.3336	67	67	22.3529
Σ Sum Earth %			100.000	
Σ Global Albedo				29.3956

349
350 Renormalization is done as follows:

- 351 1. Model starts with 1950 Table 5a albedo 29.4118%, then 2019 urban coverage area is entered.
- 352 2. For example, in Table B1, the new area increases from 0.59% to .583%. This is 0.525% larger, now
- 353 the ‘Sum of % of Earth Area’ will be 100.527% in 2019.
- 354 3. All areas are renormalized to 101.527%. For example, sea ice at 15% in 1950 becomes
- 355 $15\% \times (100.000/100.527) = 14.921\%$ and the Urban Coverage becomes $0.583\% \times (100/101.11) = 0.58\%$.

356
357 **Appendix C: Related Warming Estimates and Other Amplification Factors**

358
359 Although the results obtained here at first seem to indicate that UHIs do not appear to contribute much to global
360 warming, when other amplification factors are considered, much stronger significance will be estimated. In this
361 appendix, additional feedback factors are suggested providing a number of global warming estimates.

- 362
- 363 • *Such factors can be contentious; therefore we have chosen to provide these in this appendix mainly as*
- 364 *an aid for the reader to illustrate how climate sensitivity can factor into the magnitude of UHIs warming*
- 365 *significance. These estimates should be considered only as ballpark values.*

366
367 **C.1 Global Feedback Amplification Factors**

368
369 There is a wide range of possible estimates of climate feedback sensitivity driven by uncertainties in how water
370 vapor, clouds, and other factors change as the Earth warms. Climate feedbacks are mixed and some will amplify
371 (positive feedback) or diminish the effect of warming from the root cause effects (see for example Hausfather 2018).
372 The actual feedback is known to be positive (van Nes, 2015). Climatologists will often approximate such factors
373 frequently in reference with CO₂ doubling theory as positive. For example, water-vapor feedback alone, which is
374 one of the most important in our climate system, is thought to have the capacity to about double the direct warming
375 (Manabe and Wetherald, 1967; Randall et al., 2007, Dessler et. Al, 2008). This results from the fact that warm air
376 holds more greenhouse moisture gas. Climate models incorporate this feedback. Water vapor feedback is strongly
377 positive, with most evidence supporting a magnitude of 1.6 to 2.0 W/m²/K (Dessler et. al., 2008). Also water vapor
378 feedback is considered a faster feedback mechanism (Hansen, 2008). We will use a factor of 1.75, a bit less than a
379 doubling factor of 2. This factor would apply equally to UHI warming contribution, Greenhouse Gases (GHG), or
380 warming due to sea ice melting.

381
382 **C.2 WAASU Model Applied to the Melting of Sea Ice**

383
384 While the Antarctic sea ice has remained roughly constant, the Arctic sea ice is melting at an alarming rate of
385 12.85% in the last two decades (NASA sea ice, 2019). This apparent trend appears to yield about a 26% change in
386 sea ice loss. It is difficult to find a strong reference for quantifying global warming impact due to Arctic sea ice
387 melting. However, we might get a rough ballpark approximation by this WAASU model (and also illustrate one of
388 the strengths of the model). Sea ice melting will results in a significant albedo change roughly from ice albedo of
389 0.6, to the open ocean albedo of 0.06 (see Table C1 and C2). Fortunately, the Arctic areas receive only about 40% as

390 much solar radiation (Sciencing, 2018) reducing the feedback effect. From Equation 5, the effective sea ice surface
 391 area reduction from the irradiance decrease can be approximated as

392
 393 Effective sea ice surface area= 15% (1-0.26 x 0.40)=13.44% (a 1.56% reduction of effective area). (C-1)
 394

395 In the WAASU model, we will have to make an assumption that the effective ocean surface area increases
 396 proportionately by 1.56% to 57.56% (see Table C2). The model then finds that the global albedo change decreases
 397 from 29.4118 to 28.9948%. (Note that alternately we could have set the albedo to 29.4118% in 2019 and worked
 398 back to 1950. In this case the albedo would have increase to 29.83%).
 399

400 **Table C1.** Schneider results (Albedo=29.4118, 1950) **Table C2.** Sea ice loss - albedo change (29.0643%, 2019)

Surface	Albedo	% Area of Surface	Normalized Earth Area	Weighted Albedo %
	A	B	C=A x B x (1-0.67)	A x C
Sum of Water Type		71		
Sea Ice	0.6	15	4.95	2.970
Water	0.06	56	18.48	1.109
155Sum of Land Type		29		
Land - (UHI + Coverage)	0.3118	28.941	9.55053	2.978
UHI + Coverage	0.12	0.059	0.01947	0.002
		Σ=100.000	33.000	7.05882
			Cloud Area	
Clouds	0.3336	67	67	22.35294
Σ Sum Earth %			100.000	
Σ Global Albedo				29.4118

Surface	Albedo	Normalized % Surface Area	Normalized Earth Area	Weighted Albedo %
	A	B	C=A x B x (1-0.67)	A x C
Sum of Water Type		71		
Sea Ice	0.6	13.44	4.4352	2.507
Water	0.06	57.56	18.9948	1.14
Sum of Land Type		29	23.43	
Land - (UHI + Coverage)	0.3118	28.941	9.55053	2.978
UHI + Coverage	0.12	0.059	0.01947	0.002
		100.000	33.000	6.6395
			Cloud Area	
Clouds	0.3336	67	67	22.3530
Σ Sum Earth %			123.430	
Σ Global Albedo				29.1338

401
 402 The Global Warming (GW) is found as:

403
 404
$$\%GW = \{(P/\epsilon\sigma)^{0.25}_{2019} - (P/\epsilon\sigma)^{0.25}_{1950}\} / 0.95^{\circ}C, \quad (C-2)$$

405
 406 where P=340W/m² x (1-Albedo) and ε=1. The warming increase due to ice melting is estimated from this model to
 407 be about 0.25°C or 26.4% of the 0.95 °C increase in 2019.

408
 409 This estimate should only be taken as ballpark due to numerous uncertainties as climatologists find it hard to fully
 410 quantify the seasonal variations in ice change and to know the possible impact on cloud coverage increase from
 411 additional warming evaporation. However, one would expect less evaporation in the Arctic. Thus, there are a lot of
 412 uncertainties.

413
 414 **C.3 Ballpark Contributions to Global Warming**

415
 416 Table C3 summarizes the key global warming cause and effect factors that we have described.

417
 418 **Table C3.** Global warming factors of interest

Urban Climate Amplification	Effects	Where Applied
UHI Area Amplification Factor	3.1 UHI Amplification	Applied to 2019 UHI Area
UHI Dome Horizontal Method	2.9 UHI Amplification	Applied to 2019 UHI Area
Ice Melting	0.25°C	25 °C out of 0.95 °C
Atmospheric Moisture Increase	1.75 GW Amplification	Applied to Ice Melting Temp, UHI, and GHGs +X*

419 where X is any other feedbacks (positive or negative)

420
 421 Then major contributions to global warming can be simplified as follows

422
 423
$$\Delta T_{GW} = \lambda \Delta F = \Delta T_{UHI} + \Delta T_{Water-Vapor} + \Delta T_{Sea-Ice} + \Delta T_{GHG+X}, \quad (C-3)$$

424

425 where $\Delta T_{GW}=0.95^{\circ}\text{C}$, $\Delta T_{\text{UHI-Schneider}}=0.0147^{\circ}\text{C}$ (Table 7), $\Delta T_{\text{Sea-Ice}}=0.25^{\circ}\text{C}$, λ is the climate sensitivity, and ΔF is the
 426 radiative forcing change. We have two unknowns $\Delta T_{\text{Water-Vapor}}$ and $\Delta T_{\text{GHG+X}}$. Here X are other feedback mechanisms
 427 like increases in cloud coverage so it can be both positive or negative. These two unknowns may be estimated from
 428 the following two equations

429
 430
$$0.95^{\circ}\text{C} = \text{AF}_{\text{water vapor}} \times (\Delta T_{\text{UHI}} + \Delta T_{\text{GHG+X}} + \Delta T_{\text{Sea-Ice}}) = 1.75 (0.0147^{\circ}\text{C} + \Delta T_{\text{GHG+X}} + 0.25^{\circ}\text{C}) \quad (\text{C-4})$$

431 and

432
$$0.95^{\circ}\text{C} = \Delta T_{\text{UHI}} + \Delta T_{\text{GHG+X}} + \Delta T_{\text{Sea-Ice}} + \Delta T_{\text{Water-Vapor}} = 0.0147^{\circ}\text{C} + \Delta T_{\text{GHG+X}} + 0.25^{\circ}\text{C} + \Delta T_{\text{Water-Vapor}}. \quad (\text{C-5})$$

433
 434 The water vapor $\text{AF}_{\text{water-vapor}}=1.75$ is discussed above. Then solving, the results are tabulated in the Table C3. We
 435 note that in terms of root causes, these suggested values indicate that the UHI effect (with coverage) is responsible
 436 for between 5 to 24% of global warming.

437
 438 **Table C3. Global warming contributions (2019)**

Warming Component	Temperature Contribution (°C)	Percent of GW Root Cause	Percent of GW	Radiative Forcing W/m ²
Schneider Study				
Urbanization	0.0146	<u>5</u>	1.54	0.055
Greenhouse gases + X	0.278	95	29.3	1.5
Sea ice melting feedback	0.25		26.3	1.35
Water vapor feedback	0.4073		42.9	2.19
Total	Σ0.95			5.1
GRUMP Study				
Urbanization	0.0713	<u>24.4</u>	7.6%	0.271
Greenhouse gases + X	0.2215	75.6	23	1.19
Sea ice melting feedback	0.25		26	1.25
Water vapor feedback	0.407		43	2.19
Total	Σ0.95			4.9

439
 440 From the table the UHI effective feedback sensitivity contribution is about 3.2 (5%/1.54% or 24%/7.6%). This also
 441 indicated that the UHI area sensitivity would increase by 3.2 from 0.094 to about 0.3 W/m²/%Normalized Area (see
 442 Table 7).

443
 444 Often, we would like an estimate of the GHG effect related to CO₂. If we use a low value for the doubling
 445 temperature of 1.5°C, then $\lambda_{2\times\text{CO}_2} \approx 0.4^{\circ}\text{C}/(\text{W}/\text{m}^2)$, and then we can write

446
$$\Delta T_{\text{CO}_2+\text{X}} = \lambda \Delta F = \Delta F (\lambda_{2\times\text{CO}_2} + \lambda_{\text{X}}) = 0.278 = 1.5 (0.4 + \lambda_{\text{X}}). \quad (\text{C-6})$$

447 Results indicate that $\Delta T_{\text{CO}_2} \approx 0.6^{\circ}\text{C}$, $\Delta T_{\text{X}} = -0.32^{\circ}\text{C}$, and $\lambda_{\text{X}} = -0.214$. We reiterate that values in this appendix should
 448 only be used as crude estimated examples.

449
 450 **Appendix D: WAASU Model References**

451
 452 Table D1 provides references for the WAASU model values.

453
 454 **Table D1 Key References for WAASU model**

Parameter	Albedo (reference)	1950 Area (reference)
Sea Ice	50-70%, average 60% (NSID 2020)	15% (Lindsey 2019)
Water	0.06 (NSIDC 2020)	56% Ocean+Sea Ice=71% (USGS)
Land-(UHI+Coverage)	Adjusted to obtain 29.412% and surface reflected of 7.06 Earth Albedo in 1950 thereafter held fixed (see IPCC Hartmann (2013) AR5 report)	29%-Urban Coverage
UHI+Cov	0.12 Sugawara et. Al (2014)	See Table 1
Clouds	22.35294 (IPCC Hartmann et al., 2013)	67% (Earthobservatory, NASA)
Earth Albedo	29.412% (IPCC Hartmann, 2013)	-

455
 456

457 **References**

- 458
- 459 Barr J. M., 2019 The Economics of Skyscraper Height (Part IV): Construction Costs Around the World,
460 <https://buildingtheskyline.org/skyscraper-height-iv/>
- 461 Basara J. ,P. Hall Jr. , A.Schroeder , B.Illston ,K.Nemunaitis 2008, Diurnal cycle of the Oklahoma City urban heat
462 island, *J. of Geophysical Research*
- 463 Cao C.X. , Zhao J., P. Gong, G. R. MA, D.M. Bao, K.Tian, Wetland changes and droughts in southwestern China,
464 *Geomatics, Natural Hazards and Risk*, Oct 2011,
465 <https://www.tandfonline.com/doi/full/10.1080/19475705.2011.588253>
- 466 Cormack L. 2015 Where does all the stormwater go after the Sydney weather clears? The Sydney Morning Herald,
467 [https://www.smh.com.au/environment/where-does-all-the-stormwater-go-after-the-sydney-weather-clears-](https://www.smh.com.au/environment/where-does-all-the-stormwater-go-after-the-sydney-weather-clears-20150430-1mx4ep.html)
468 [20150430-1mx4ep.html](https://www.smh.com.au/environment/where-does-all-the-stormwater-go-after-the-sydney-weather-clears-20150430-1mx4ep.html)
- 469 Dessler A. E. ,Zhang Z., Yang P., Water-vapor climate feedback inferred from climate fluctuations, 2003–2008,
470 *Geophysical Research Letters*, (2008), <https://doi.org/10.1029/2008GL035333>
- 471 Earthobservatory, NASA (clouds albedo 0.67) <https://earthobservatory.nasa.gov/images/85843/cloudy-earth>
- 472 Fan, Y., Li, Y., Bejan, A. *et al.* Horizontal extent of the urban heat dome flow. *Sci Rep* 7, 11681 (2017).
473 <https://doi.org/10.1038/s41598-017-09917-4>
- 474 Feddema, J. J., K. W. Oleson, G. B. Bonan, L. O. Mearns, L. E. Buja, G. A. Meehl, and W. M. Washington (2005),
475 The importance of land-cover change in simulating future climates, *Science*, **310**, 1674– 1678,
476 doi:10.1126/science.1118160
- 477 Galka M. 2016, Half the World Lives on 1% of Its Land, Mapped, [https://www.citylab.com/equity/2016/01/half-](https://www.citylab.com/equity/2016/01/half-earth-world-population-land-map/422748/)
478 [earth-world-population-land-map/422748/](https://www.citylab.com/equity/2016/01/half-earth-world-population-land-map/422748/), (2016 publication on 2000 data set, [http://metrocosm.com/world-](http://metrocosm.com/world-population-split-in-half-map/)
479 [population-split-in-half-map/](http://metrocosm.com/world-population-split-in-half-map/)
- 480 Global Rural Urban Mapping Project (GRUMP) 2005, Columbia University Socioeconomic Data and Applications
481 Center, Gridded Population of the World and the Global Rural-Urban Mapping Project (GRUMP).
- 482 Hansen, J., "2008: Tipping point: Perspective of a climatologist." Archived 2011-10-22 at the Wayback Machine,
483 Wildlife Conservation Society/Island Press, 2008. Retrieved 2010.
- 484 Hartmann, D.L., A.M.G. Klein Tank, M. Rusticucci, L.V. Alexander, S. Brönnimann, Y. Charabi, F.J. Dentener,
485 E.J. Dlugokencky, D.R. Easterling, A. Kaplan, B.J. Soden, P.W. Thorne, M. Wild and P.M. Zhai, 2013:
486 Observations: Atmosphere and Surface. In: *Climate Change 2013: The Physical Science Basis. Contribution of*
487 *Working Group I to the Fifth Assessment Report of the Intergovernmental Panel on Climate Change* [Stocker,
488 T.F., D. Qin, G.-K. Plattner, M. Tignor, S.K. Allen, J. Boschung, A. Nauels, Y. Xia, V. Bex and P.M. Midgley
489 (eds.)]. Cambridge University Press, Cambridge, United Kingdom and New York, NY, USA.
- 490 Hirshi M. ,Seneviratne S. , V. Alexandrov, F. Boberg, C. Boroneant, O. Christensen, H. Formayer, B. Orlowsky &
491 P. Stepanek, Observational evidence for soil-moisture impact on hot extremes in Europe, *Nature Geoscience* 4,
492 17-21 (2011)
- 493 Huang Q. , Lu Y. 2015 Effect of Urban Heat Island on Climate Warming in the Yangtze River Delta Urban
494 Agglomeration in China, *Intern. J. of Environmental Research and Public Health* 12 (8): 8773 (30%)
- 495 Jones, P. D., D. H. Lister, and Q.-X. Li, 2008: Urbanization effects in large-scale temperature records, with an
496 emphasis on China. *J. Geophys. Res.*, 113, D16122, doi: 10.1029/2008JD009916.
- 497 Lindsey R, Scott M., (2019), *Climate Change: Arctic Sea Ice Summer Minimum*, NOAA Climate.gov,
498 <https://www.climate.gov/news-features/understanding-climate/climate-change-minimum-arctic-sea-ice-extent>
- 499 Manabe, S., and R. T. Wetherald (1967), Thermal equilibrium of atmosphere with a given distribution of relative
500 humidity, *J. Atmos. Sci.*, 24, 241–259.
- 501 McKittrick R. and Michaels J. 2004. A Test of Corrections for Extraneous Signals in Gridded Surface Temperature
502 Data, *Climate Research*
- 503 McKittrick R., Michaels P. 2007 Quantifying the influence of anthropogenic surface processes and inhomogeneities
504 on gridded global climate data, *J. of Geophysical Research-Atmospheres*
- 505 McKittrick Website Describing controversy: <https://www.rossmckittrick.com/temperature-data-quality.html>
- 506 NASA 1900-2006 updated, 2020 <https://climate.nasa.gov/vital-signs/global-temperature/>
- 507 NASA 2000, Gridded population of the world, , [https://sedac.ciesin.columbia.edu/data/set/gpw-v3-population-](https://sedac.ciesin.columbia.edu/data/set/gpw-v3-population-count/data-download)
508 [count/data-download](https://sedac.ciesin.columbia.edu/data/set/gpw-v3-population-count/data-download)
- 509 NASA Sea Ice, (2019) <https://climate.nasa.gov/vital-signs/arctic-sea-ice/>
- 510 NSID 2020, National Snow & Ice Data Center, "Thermodynamics: Albedo". [nsidc.org](https://nsidc.org/cryosphere/seaice/processes/albedo.html). Retrieved 14 August 2016.
511 <https://nsidc.org/cryosphere/seaice/processes/albedo.html>
- 512 Randall, D. A. et al. (2007), Climate models and their evaluation, in *Climate Change 2007: The Physical Science*
513 *Basis. Contributions of Working Group I to the Fourth Assessment Report of the Intergovernmental Panel on*
514 *Climate Change*, edited by S. Solomon et al., pp. 591–662, Cambridge Univ. Press, Cambridge, U.K.
- 515 Ren, G.; Chu, Z.; Chen, Z.; Ren, Y. 2007 Implications of temporal change in urban heat island intensity observed at
516 Beijing and Wuhan stations. *Geophys. Res. Lett.* , 34, L05711,doi:10.1029/2006GL027927.
- 517 Ren, G.-Y., Z.-Y. Chu, J.-X. Zhou, et al., (2008): Urbanization effects on observed surface air temperature in North
518 China. *J. Climate*, 21, 1333-1348

- 519 Schmidt G. A. 2009 Spurious correlations between recent warming and indices of local economic activity, *Int. J. of*
520 *Climatology*
- 521 Schneider, A., M. Friedl, and D. Potere, 2009: A new map of global urban extent from MODIS satellite data.
522 *Environmental Research Letters*, 4(4), 044003, doi:10.1088/1748-9326/4/4/044003
- 523 Satterthwaite D.E., F. Aragón-Durand, J. Corfee-Morlot, R.B.R. Kiunsi, M. Pelling, D.C. Roberts, and W. Solecki,
524 2014: Urban areas. In: *Climate Change 2014: Impacts, Adaptation, and Vulnerability. Part A: Global and*
525 *Sectoral Aspects. Contribution of Working Group II to the Fifth Assessment Report of the Intergovernmental*
526 *Panel on Climate Change (IPCC)*
- 527 Sciencing (2018) <https://sciencing.com/sun-intensity-vs-angle-23529.html>
- 528 Stone B. 2009 Land use as climate change mitigation, *Environ. Sci. Technol.*, 43(24), 9052–9056,
529 doi:10.1021/es902150g
- 530 Sugawara, H., Takamura, T. Surface Albedo in Cities (0.12): Case Study in Sapporo and Tokyo, Japan. *Boundary-*
531 *Layer Meteorol* **153**, 539–553 (2014). <https://doi.org/10.1007/s10546-014-9952-0>
- 532 US Population Growth 1900-2006, u-s-history.com/pages/h980.html
- 533 USGS 1900-2006, Materials in Use in U.S. Interstate Highways, <https://pubs.usgs.gov/fs/2006/3127/2006-3127.pdf>
- 534 USGS on Amount of Earth covered by water, [https://www.usgs.gov/special-topic/water-science-](https://www.usgs.gov/special-topic/water-science-school/science/how-much-water-there-earth?qt-science_center_objects=0#qt-science_center_objects)
535 [school/science/how-much-water-there-earth?qt-science_center_objects=0#qt-science_center_objects](https://www.usgs.gov/special-topic/water-science-school/science/how-much-water-there-earth?qt-science_center_objects=0#qt-science_center_objects)
- 536 van Nes E. H., Scheffer M., Brovkin V., Lenton T. M., Ye H, Deyle E. and Sugihara G., *Nature Climate Change*
537 2015. [dx.doi.org/10.1038/nclimate2568](https://doi.org/10.1038/nclimate2568)
- 538 World Bank, 2018 population growth rate, worldbank.org
- 539 Yang, X.; Hou, Y.; Chen, B. 2011 Observed surface warming induced by urbanization in east China. *J. Geophys.*
540 *Res. Atmos*, 116, doi:10.1029/2010JD015452.
- 541 Zhang, X., Friedl, M. A., Schaaf, C. B., Strahler, A. H. & Schneider, A. 2004 The footprint of urban climates on
542 vegetation phenology. *Geophys. Res. Lett.* **31**, L12209
- 543 Zhao, Z.-C., 1991: Temperature change in China for the last 39 years and urban effects. *Meteorological Monthly* (in
544 Chinese), 17(4), 14-17.
- 545 Zhao, Z.-C., 2011: Impacts of urbanization on climate change. in: 10,000 Scientific Difficult Problems: Earth
546 Science, 10,000 scientific difficult problems Earth Science Committee Eds., Science Press, 843-846. 30%
- 547 Zhao L, Lee X, Smith RB, Oleson K, Strong 2014, contributions of local background climate to urban heat islands,
548 *Nature*. 10;511(7508):216-9. doi: 10.1038/nature13462
- 549 Zhou D. , Zhao S. , L. Zhang, G Sun and Y. Liu, 2015, The footprint of urban heat island effect in China, *Scientific*
550 *Reports*. 5: 11160
- 551 Zhou Y. , Smith S. , Zhao K. , M. Imhoff, A. Thomson, B. Lamberty, G. Asrar, X. Zhang, C. He and C. Elvidge, A
552 global map of urban extent from nightlights, *Env. Research Letters*, 10 (2015), (study uses a 2000 data set).

556 Conflicts of Interest

557 The author declares that he has no conflicts of interest.

558